Critical behavior at paramagnetic to ferromagnetic phase transition in $Pr_{0.5}Sr_{0.5}MnO_3$: A bulk magnetization study

A. K. Pramanik and A. Banerjee
UGC-DAE Consortium for Scientific Research, University Campus, Khandwa Road, Indore 452001, Madhya Pradesh, India
(Received 7 April 2009; published 22 June 2009)

The critical behavior at the paramagnetic to ferromagnetic phase transition in $Pr_{0.5}Sr_{0.5}MnO_3$ is studied using techniques such as modified Arrott plot, Kouvel-Fisher plot, and critical isotherm analysis. Though the nature of this transition is found to be of second order, the estimated critical exponents β, γ, and δ are in between the theoretically predicted values for three-dimensional Heisenberg and mean-field interaction models. However, it is noteworthy that the scaling relations are obeyed indicating renormalization of interactions around the Curie temperature (T_C). Temperature variation in effective exponents (β_{eff} and γ_{eff}) resemble with those for disordered ferromagnet. It is shown that fully localized-spin interaction models are not applicable for this compound, and ferromagnetic interaction has itinerant character. Moreover, the exponents determined in this study are close to those calculated from the results of renormalization group approach for a heuristic model of two-dimensional Heisenberg spins coupled with long-range interaction. These results suggest that critical phenomenon in $Pr_{0.5}Sr_{0.5}MnO_3$, which is found to be an inhomogeneous ferromagnet around T_C, could not be described within the framework of existing universality classes and probably belong to a separate class.

DOI: 10.1103/PhysRevB.79.214426 PACS number(s): 75.40.Cx, 75.47.Lx, 75.30.Kz

I. INTRODUCTION

Changes in physical properties across the paramagnetic (PM)-ferromagnetic (FM) phase transition are one of the vital issues related to both physics and functionality of perovskite manganites with generic formula $R_{1-x}A_xMnO_3$ (where R and A represents trivalent rare earth and divalent alkaline earth element, respectively). Two basic questions related to this phase transition are: (i) the order of the phase transition, and (ii) the universality class based on the dimensionality of lattice (d) and the dimensionality of order parameter (n). At present, no consensus or comprehensive understanding exists on either of these issues in manganites. For example, systems having large R/A site average ionic radii ($\langle r_A \rangle$) like $La_{1-x}Sr_xMnO_3$ are characterized with second order PM-FM phase transition.[1,2] On the contrary, the PM-FM transition in $La_{1-x}Ca_xMnO_3$ having smaller $\langle r_A \rangle$ is proved to be of first-order type from various techniques.[3,4] However, a notable exception is $La_{0.67}Mg_{0.33}MnO_3$ having much smaller $\langle r_A \rangle$ shows second order PM-FM phase transition.[5] Similarly, there exists ambiguity regarding the renormalization of interaction around critical point which is governed by the universality class. In this correlated electron system, ferromagnetism usually arises from the coupling of itinerant e_g electrons with the localized t_{2g} electrons dictated by double exchange (DE) interaction.[6] In earlier theoretical work, critical phenomenon related to transition from PM to FM state in manganite has been described within framework of long-range mean-field theory.[7] However, the recent theoretical calculations have predicted the critical exponents in manganites in agreement with the short-range exchange interaction model.[8,9]

In real system, much more complex situation is encountered. Critical exponents for manganites show large variation which cover almost all the universality classes, even for the similar system when different experimental tools are used to determine them (See Table I in Ref. 1). Manganites are intrinsically inhomogeneous both above and below PM-FM transition temperature (T_C).[10,11] Thus, it is unlikely that the renormalization of interaction around the critical point will follow the scaling relations with critical exponents belonging to the conventional universality classes. The experimentally estimated exponents for different inhomogeneous perovskite systems are also found to be incompatible with the existing universality classes.[12–14] The presence of Griffiths phase like singularities[15] in manganites further complicates the situation. Recently, new scaling relation has been proposed for FM-Griffiths phase transition, and the same has been verified from the experimental data on manganite.[16]

The critical behavior across PM-FM phase transition in half-doped $Pr_{0.5}Sr_{0.5}MnO_3$ (PSMO) is studied here. This compound is an important member in manganite family having intermediate one electron bandwidth and, to the best of our knowledge, this study is first of its kind for this system. PSMO has PM-FM transition followed by FM to A-type antiferromagnet (AF) transition at lower temperature (T_N).[17,18] This composition lies at the boundary of FM and AF phase,[19] resulting in many important consequences such as coexistence of tunable fraction of equilibrium AF insulating (I) phase with higher entropy FM metallic (M) phase at low temperature (T).[20] It has been recently shown that just below T_C, AF clusters evolve within FM phase in PSMO.[21] Moreover, FM interaction extends much above T_C which is also evident in single crystal of this compound.[21,22] Hence, all these above mentioned uncommon features will have nontrivial consequences on critical behavior of this system. For example, though we have found PM-FM transition in PSMO is second order but the determined critical exponents (β, γ, and δ) do not belong to any conventional universality classes and they are in between the values theoretically predicted for three-dimensional (3D) Heisenberg and mean-field interaction model. However, it is rather significant that the interactions get renormalized around T_C and exponents obey scaling relations. The effective exponents (β_{eff} and γ_{eff}) vary with

temperature similar to those for disordered FM. The FM interaction does not satisfy the localized model and has certain amount of itinerant character. The estimated exponents in this study are close to the values which are calculated from renormalization group approach[23] for two-dimensional (2D) Heisenberg FM combined with long-range interaction. This scenario is probably justified for this compound as its ground state is having A-type AF where FM planes are coupled antiferromagnetically accompanied by 2D metallic mobility of e_g electrons along the planes.

II. EXPERIMENTAL DETAILS

Polycrystalline sample $Pr_{0.5}Sr_{0.5}MnO_3$ has been prepared by the standard solid state ceramic route. Rietveld analysis of x-ray diffraction data shows that the sample is in single phase. The atomic concentration in sample is checked through selective area energy dispersive analysis of x-ray (EDAX) attached with transmission electron microscope (Model: Tecnai 20 G2). Oxygen stoichiometry is verified from iodometric titration with the samples taking from different parts of a pellet. The results show that sample is chemically homogeneous, stoichiometric, and around half doping to the accuracy of experimental techniques. Details of sample preparation and characterization techniques are given in Ref. 21. Magnetization (M) measurements have been carried out with Quantum Design 14 Tesla Vibrating Sample Magnetometer (PPMS-VSM). Isotherms are collected at an interval of 0.2 K around T_C. For proper stabilization of temperature, 20 min wait time is given before recording each isotherm. The external applied magnetic field (H_a) has been corrected for the demagnetization effect to get the internal field H_i [$=H_a$-$NM(T,H_a)$, where M is the measured magnetization]. Demagnetization constant (N) has been calculated from the low field M vs H plot following the method given in Ref. 21. The calculated H_i has been used for scaling analysis.

III. SCALING ANALYSIS

According to the scaling hypothesis, for second order phase transition the spontaneous magnetization $M_S(T)$ below T_C, inverse initial susceptibility $\chi_0^{-1}(T)$ above T_C and magnetization M at T_C shows following power-law dependence:[24]

$$M_S(T) = M_0(-\epsilon)^{\beta}, \quad \epsilon < 0, \tag{1}$$

$$\chi_0^{-1}(T) = \Gamma(\epsilon)^{\gamma}, \quad \epsilon > 0, \tag{2}$$

$$M = XH^{1/\delta}, \quad \epsilon = 0, \tag{3}$$

where M_0, Γ and X are the critical amplitudes; β, γ, and δ are the critical exponents; and $\epsilon=(T-T_C)/T_C$ is the reduced temperature. The magnetic equation of state is a relationship among the variables $M(H,\epsilon)$, H, and T. Using scaling hypothesis this can be expressed as:

$$M(H,\epsilon) = \epsilon^{\beta} f_{\pm}\left(\frac{H}{\epsilon^{\beta+\gamma}}\right), \tag{4}$$

where $f_+(T>T_C)$ and $f_-(T<T_C)$ are the regular functions. In terms of renormalized magnetization $m \equiv \epsilon^{-\beta}M(H,\epsilon)$ and

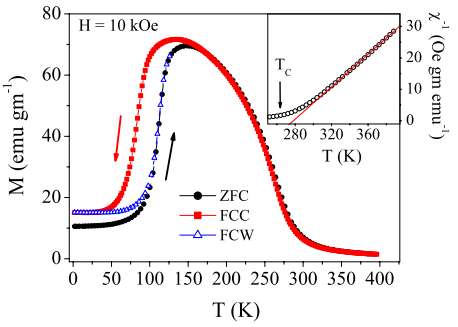

FIG. 1. (Color online) Temperature variation in magnetization measured in 10 kOe field following ZFC, FCC, and FCW protocol (defined in text). In inset inverse susceptibility measured in 10 kOe is plotted as a function of temperature. The straight line is due to Curie-Weiss law fitting of susceptibility data above T_C.

renormalized field $h \equiv \epsilon^{-(\beta+\gamma)}H$, the Eq. (4) can be written as

$$m = f_{\pm}(h). \tag{5}$$

Equation (5) implies that for true scaling relations and right choice of β, γ, and δ values, scaled m plotted as a function of scaled h will fall on two universal curves: one above T_C and another below T_C. This is an important criterion for critical regime.

Usually, exponents in the asymptotic regime ($\epsilon \to 0$) show universal properties (i.e, they depend only on the global parameters of system like symmetry, dimensionality of the order parameter and the space etc., and are independent of microscopic details of the sample). However, exponents often show various systematic trends or *crossover* phenomenon as one approaches T_C.[25,26] This occurs due to the presence of various competing couplings and/or disorder. For this reason, it is useful to introduce temperature-dependent *effective exponents* for $\epsilon \neq 0$. It can be mentioned that effective exponents are nonuniversal properties, and they are defined as:

$$\beta_{\text{eff}}(\epsilon) = \frac{d[lnM_S(\epsilon)]}{d(ln\epsilon)}, \quad \gamma_{\text{eff}}(\epsilon) = \frac{d[ln\chi_0^{-1}(\epsilon)]}{d(ln\epsilon)}. \tag{6}$$

In the asymptotic limit, effective exponents approach universal exponents.

IV. RESULTS AND DISCUSSIONS

Figure 1 shows the temperature variation in magnetization measured in 10 kOe field following zero field cooled (ZFC), field cooled cooling (FCC), and field cooled warming (FCW) protocol. This compound shows PM-FM transition at higher temperature and FM-AF at lower temperature.[17,21] The rounded nature of PM-FM transition in figure arises due to high-measuring field whereas in low field this transition is reasonably sharp.[21] Similarly, due to high-field FM-AF transition occurs at low T in Fig. 1, but in low field this transition shifts to higher T as shown in Ref. 20. Figure 1 clearly shows that FM-AF transition is accompanied with huge thermal hysteresis, which is an indication of first-order phase transition. However, there is no distinguishable thermal hysteresis around PM-FM transition, qualitatively suggesting it to

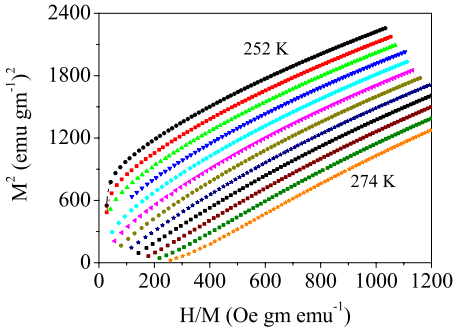

FIG. 2. (Color online) Arrott plot (M^2 vs H/M) of isotherms which are collected at close temperature interval around T_C for $Pr_{0.5}Sr_{0.5}MnO_3$. Only few representative isotherms are shown for clarity.

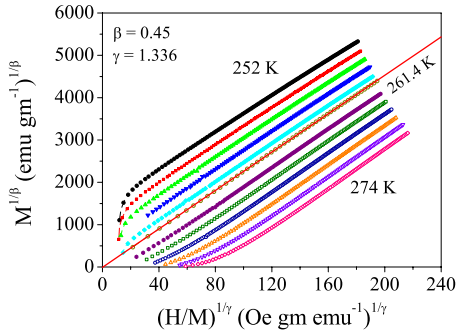

FIG. 3. (Color online) Modified Arrott plot ($M^{1/\beta}$ vs $(H/M)^{1/\gamma}$) of isotherms with β=0.45 and γ=1.336 for $Pr_{0.5}Sr_{0.5}MnO_3$. The straight line is linear fit of isotherm at 261.4 K which passes through origin. Only a few representative isotherms are shown for clarity.

be a second order in nature. The inset of Fig. 1 plots $(\chi=M/H)^{-1}$ vs T, showing Curie-Weiss law is obeyed only at high T. The close observation of this figure reveals that χ^{-1} deviates from straight line behavior around 320 K which is much higher than T_C. Moreover, Weiss temperature obtained from this plot is 278 K, and this value is reasonably higher than T_C. These indicate the presence of FM spin interaction above T_C.

A. Arrott plot

Conventional method to determine the critical exponents and critical temperature involves the use of Arrott plot.[27] According to this method, isotherms plotted in the form of M^2 vs H/M constitute a set of parallel straight lines around T_C. It can be mentioned that Arrott plot assumes the critical exponents following mean-field theory (β=0.5 and γ=1). Hence, linear behavior of isotherms in high field indicates the presence of mean-field interactions. The advantages of this plot are that (i) T_C can be determined accurately, since the isotherm at T_C will pass through the origin; (ii) it directly gives $\chi_0^{-1}(T)$ as an intercept on H/M axis; (iii) intercept on positive M^2 axis gives $M_S(T)$. Figure 2 shows the Arrott plot of this compound around T_C. However, all the curves in this plot show nonlinear behavior having downward curvature even in high field indicating non-mean-field-like behavior. Moreover, the concave downward curvature clearly indicates second-order phase transition according to the criterion suggested by Banerjee.[28] This criterion has been explicitly used in other manganites to identify the order of phase transition.[4]

Thus, PSMO has second-order phase transition and to characterize this we have taken recourse to which is commonly known as modified Arrott plot.[29] This is given by following equation of state:

$$\left(\frac{H}{M}\right)^{1/\gamma} = a\frac{(T-T_C)}{T} + bM^{1/\beta}, \tag{7}$$

where a and b are considered to be constants. Figure 3 shows modified Arrott plot following Eq. (7) for this compound at different temperatures. This plot clearly shows the isotherms are a set of parallel straight lines in high fields which are achieved by proper selection of β and γ. However, this selection of exponents in Fig. 3 is a nontrivial task because two free parameters, namely, β and γ are involved in Eq. (7) which can lead to unphysical fitting and systematic errors in exponent values. To overcome this difficulty a rigorous iterative method has been followed to find out the proper values of β and γ. In this method starting trial values of β and γ are taken to be values for theoretical 3D Heisenberg model. These values of β and γ are substituted in Eq. (7) and figure similar to Fig. 3 is generated. Linear extrapolation of the isotherms are then taken from the high field which gives $(M_S)^{1/\beta}$ and $(\chi_0^{-1})^{1/\gamma}$ as an intercept on $M^{1/\beta}$ and $(H/M)^{1/\gamma}$ axis, respectively. These values of $M_S(T)$ and $\chi_0^{-1}(T)$ have been used to fit in Eqs. (1) and (2), respectively. According to Eq. (1), slope of the straight line fitting of $\log[M_S(T)]$ vs $\log(\epsilon)$ gives new value of β. Similarly, straight line fitting of $\log[\chi_0^{-1}(T)]$ vs $\log(\epsilon)$ according to Eq. (2) gives new γ. It can be mentioned that while fitting the straight lines, the free parameter T_C in Eqs. (1) and (2) is so adjusted that it yields best fitting. These new values of β and γ are again used to construct new modified Arrott plot (similar to Fig. 3). This process was continued till the stable values of β, γ, and T_C are achieved. After doing this exercise, a set of reasonably good parallel straight lines in Fig. 3 have been generated with the values β=0.45 and γ=1.336. It is evident in Fig. 3 that at lower field these lines are curved, as they are averaged over domains which are magnetized in different directions.[30] However, in high fields all isotherms are set of parallel straight lines. Isotherm passes through the origin is at 261.4 K which is the T_C. The finally obtained $M_S(T)$ and $\chi_0^{-1}(T)$ are plotted as a function of temperature in Fig. 4. Using these values of $M_S(T)$ and $\chi_0^{-1}(T)$, Eq. (1) gives β=0.443(2), T_C =261.44(4) and Eq. (2) gives γ=1.339(6), T_C=261.29(5). The exponents are summarized in Table I. These estimated critical exponents and T_C from Eqs. (1) and (2) are reasonably close to the values obtained from modified Arrott plot in Fig. 3 (β=0.45, γ=1.336, and T_C=261.4 K).

B. Kouvel-Fisher plot

To determine the critical exponents as well as T_C more accurately, we have analyzed the $M_S(T)$ and $\chi_0^{-1}(T)$ data by Kouvel-Fisher (KF) plot.[31] According to this method,

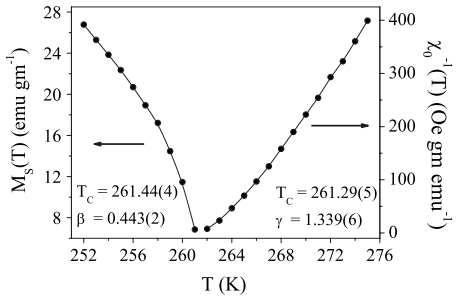

FIG. 4. Temperature variation in spontaneous magnetization $M_S(T)$ (left axis) and inverse initial susceptibility $\chi_0^{-1}(T)$ (right axis) which are obtained from the high-field extrapolation of modified Arrott plot in Fig. 3. The T_C and exponent values are obtained from straight line fitting of Eqs. (1) and (2).

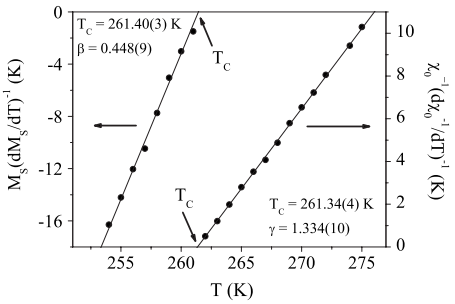

FIG. 5. Kouvel-Fisher plot of spontaneous magnetization M_S (left axis) and inverse initial susceptibility χ_0^{-1} (right axis) for $Pr_{0.5}Sr_{0.5}MnO_3$. Straight lines are due to linear fitting of data. The T_C and exponents are obtained from fitted straight lines in this plot.

$M_S(dM_S/dT)^{-1}$ vs T and $\chi_0^{-1}(d\chi_0^{-1}/dT)^{-1}$ vs T yield straight lines with slopes $1/\beta$ and $1/\gamma$, respectively. The best part of KF plot is that no prior knowledge of T_C is required as the intercept of such fitted straight lines on temperature axis is equal to T_C. The KF plot for this sample has been presented in Fig. 5. From the fitted straight lines estimated exponents and T_C are β=0.448(9), T_C=261.40(3) and γ=1.334(10), T_C=261.34(4). It is remarkable that values of critical exponents as well as T_C calculated using both modified Arrott plot and Kouvel-Fisher plot match reasonably well (see Table I). This suggests that the estimated values are self consistent and unambiguous.

C. Critical isotherm analysis

Figure 6 shows critical isotherm $M(H, T_C$=261.4 K) vs H plot, and in inset the same plot has been presented in log-log scale. According to Eq. (3), log(M) vs log(H) plot would give a straight line with slope $1/\delta$. From the linear fitting in inset of Fig. 6, we have got δ=3.955(1) (Table I). Furthermore, exponent δ has also been calculated from Widom scaling relation according to which critical exponents β, γ, and δ are related in following way:[32]

$$\delta = 1 + \frac{\gamma}{\beta} \tag{8}$$

Using the β and γ values calculated in Figs. 4 and 5, Eq. (8) yields δ=4.022(3) and 3.977(6), respectively. It is noteworthy that these values are very close to the value [3.955(1)] obtained from critical isotherm in Fig. 6. Hence, estimated exponents (β and γ) in present study are self-consistent and an accurate estimate within experimental precision.

D. Conformity of Scaling law

All these critical exponents derived from various methods are given in Table I along with the theoretically predicted values for different models. It is clear from Table I that these values do not match with the conventional universality classes. Hence, it is important to check if these critical exponents can generate the scaling equation of state (Eq. (5)) for this system. Following Eq. (5), scaled m vs scaled h has been plotted in Fig. 7 taking critical exponents β, γ, and critical temperature T_C from Table I. Inset of Fig. 7 shows the same plot on log-log scale. It is rather significant that all the data collapse into two separate branches: one below T_C and another above T_C. The reliability of the exponents and T_C has been further ensured with more rigorous method by plotting m^2 vs h/m.[33] Fig. 8 shows such plot where it is observed that all data collapse into two separate curves: one below T_C and other above T_C. This clearly indicates that the interactions get properly renormalized in critical regime following scaling equation of state.

E. Effective critical exponents

Even though estimated critical exponents in present study strictly do not belong to the common universality classes, it

TABLE I. Values of the exponents β, γ, and δ as determined from the modified Arrott plots, Kouvel-Fisher plot, and the critical isotherm are given for $Pr_{0.5}Sr_{0.5}MnO_3$. The theoretically predicted values of exponents for various universality classes are given for the sake of comparison.

Composition	Ref.	Technique	α	β	γ	δ
$Pr_{0.5}Sr_{0.5}MnO_3$	This work	Modified Arrott plot		0.443 ± 0.002	1.339 ± 0.006	4.022 ± 0.003 [a]
		Kouvel-Fisher method		0.448 ± 0.009	1.334 ± 0.010	3.977 ± 0.006 [a]
		Critical isotherm				3.955 ± 0.001
Mean Field Model	33	Theory	0.0	0.5	1.0	3.0
3D Heisenberg Model	33	Theory	−0.115	0.365	1.386	4.80
3D Ising Model	33	Theory	0.11	0.325	1.241	4.82

[a]Calculated from Widom scaling relation $\delta = 1 + \gamma/\beta$

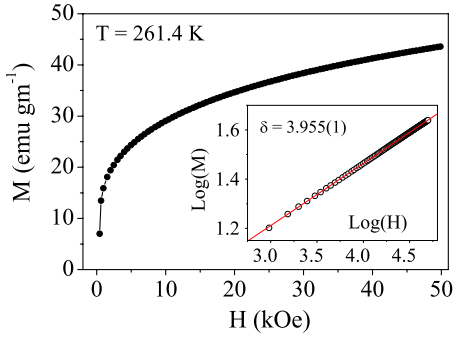

FIG. 6. (Color online) M vs H plot collected at 261.4 K(=T_C) for $Pr_{0.5}Sr_{0.5}MnO_3$. Inset shows the same plot in log-log scale and the straight line is the linear fit following Eq. (3). The critical exponent mentioned in graph are obtained from fitting of the data.

is important to find out whether they match with any universality classes as they approach asymptotic values. For this purpose, effective critical exponents (β_{eff} and γ_{eff}) have been calculated as a function of ϵ following Eq. (6). These exponents are plotted in Figs. 9(a) and 9(b). As observed in figure, both β_{eff} and γ_{eff} show nonmonotonic change with ϵ where β_{eff} shows slight dip (at $\epsilon \approx -4.3 \times 10^{-3}$) and γ_{eff} shows peak (at $\epsilon \approx 2.5 \times 10^{-2}$) and then dip (at $\epsilon \approx 2.9 \times 10^{-3}$) before approaching asymptotic regime ($\epsilon \to 0$). The lowest investigated $\epsilon(\epsilon_{\text{min}})$ are 9.18×10^{-4} and 6.12×10^{-4} for β_{eff} and γ_{eff}, respectively. It can be mentioned that β_{eff} and γ_{eff} at ϵ_{min} do not match with any predicted universality classes. We even tried to plot the scaling equation (similar to Figs. 7 and 8) with γ_{eff} (1.28), β_{eff} (0.45) at ϵ_{min}, and the data do not fully collapse into two separate branches. This probably arises from three reasons: (i) ϵ_{min} does not fall into asymptotic regime and T_C has to be approached more closely for having asymptotic exponents; (ii) ϵ_{min} is in asymptotic region as disagreement of effective exponents with universality classes in asymptotic regime is also observed in disordered materials (see Ref. 34); (iii) system goes through crossover regime to another universality class in asymptotic regime.[26] However, temperature variation in effective exponents in Fig. 9 resemble with that for disordered FM. For example, $\gamma_{\text{eff}}(\epsilon)$ shows peak for amorphous FM, whereas in

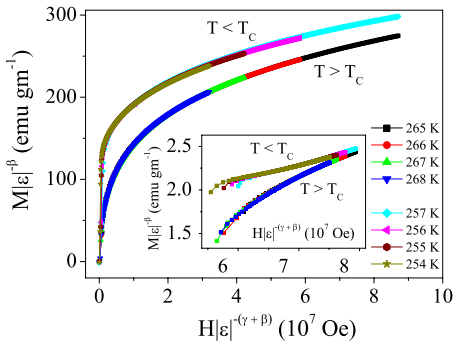

FIG. 7. (Color online) The renormalized magnetization is plotted as a function of renormalized field following Eq. (5) with T_C =261.4 K, and β, γ from Table I for $Pr_{0.5}Sr_{0.5}MnO_3$. The plot shows all the data collapse into two distinct branches: one below T_C and another above T_C. Inset shows the same plot on log-log scale.

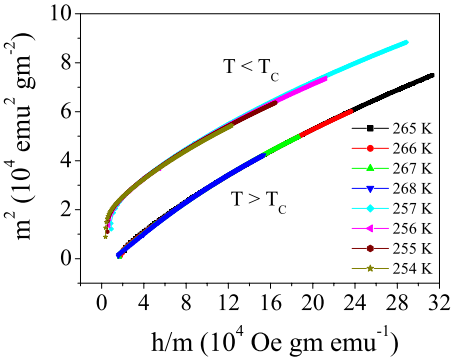

FIG. 8. (Color online) The renormalized magnetization and field (defined in text) are plotted in the form of m^2 vs h/m for $Pr_{0.5}Sr_{0.5}MnO_3$. The plot shows all the data collapse into two separate branches: one below T_C and another above T_C.

case of crystalline FM γ_{eff} decreases monotonically with increasing ϵ.[33] Recent theoretical study[34] for Heisenberg like FM has predicted that γ_{eff} remains unaffected to disorder in asymptotic regime but with introduction of disorder, γ_{eff} goes through peak at higher ϵ similar to Fig. 9(b). Similar peak in γ_{eff} has also been observed for partially frustrated amorphous alloys.[25] Thus, this study shows the presence of disorder which influences the critical behavior in this system. The disorder probably arises from dissimilar ions (Pr^{3+}, Sr^{2+}) at R/A site of perovskite structure and/or inhomogeneous phases above and below T_C, and both these are intrinsic to this system.[21]

F. Itinerant nature of FM in $Pr_{0.5}Sr_{0.5}MnO_3$

Considering the inconsistency of estimated exponents with the localized models (Table I), the nature of ferromagnetism in this compound is examined from Rhodes-

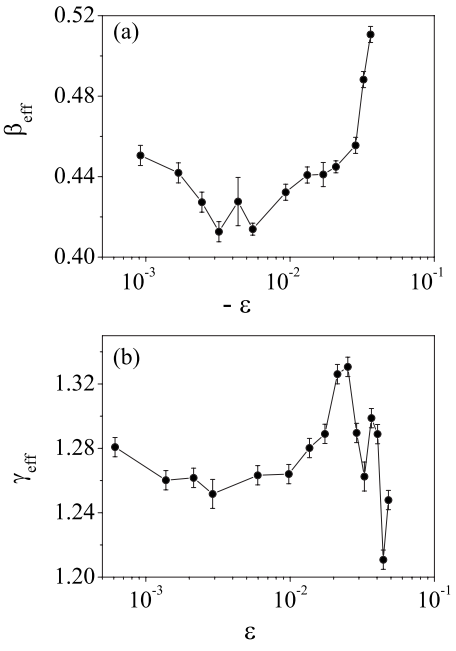

FIG. 9. Effective exponents (a) β_{eff} below T_C and (b) γ_{eff} above T_C are plotted as a function of reduced temperature ϵ [$=(T - T_C)/T_C$] for $Pr_{0.5}Sr_{0.5}MnO_3$.

Wohlfarth criterion.[35] This is used to distinguish between the localized model and the itinerant model for FM based on the ratio of number of magnetic carriers per atom deduced from low-T saturation magnetization (q_s) with that calculated from effective Curie-Weiss constant above T_C(q_c).[36] For the localized model, saturation magnetization equals to the fully aligned spin only moment giving rise to q_c/q_s ratio equal to unity. On the other hand, for itinerant model the saturation magnetization is less than the fully aligned spin moment, resulting in $q_c/q_s > 1$. For PSMO, q_s is calculated from saturation moment measured at 150 K (in its FM state), and the value is 3.07. The q_c has been calculated from effective PM moment (p_{eff}) which is obtained from Curie-Weiss law.[37] Considering $p_{\text{eff}} = g\sqrt{S(S+1)}$, where $S(=q_c/2)$ is effective spin per atom, q_c has been determined to be 4.62. This measured value of q_c for PSMO is higher than the expected spin only value (3.5) for half-doped manganite. This implies the presence of FM spin clusters above T_C.[21] Moreover, the upward deviation of $\chi^{-1}(T)$ from Curie-Weiss behavior above T_C, as observed in inset of Fig. 1, also suggests the existence of spin clusters in this compound above T_C.[11] Thus, the q_c/q_s ratio becomes >1 indicating itinerant character of FM in this compound.

G. Spin interaction in $Pr_{0.5}Sr_{0.5}MnO_3$

It is clear from the earlier sections that FM interaction in PSMO has the following properties: (i) it does not comply with the 3D short-range interaction models; (ii) estimated exponents are in between the values for 3D Heisenberg and mean-field model indicating interaction is of extended type; (iii) it is having of itinerant character. Hence, it is important to understand the nature as well as the range of interaction in this compound. The extended type of interaction can arise either from dipole-dipole interaction[38] or isotropic interaction between spins which decays in d-dimension as $J(r) \sim r^{-(d+\sigma)}$, where r is the distance and σ is the range of interaction.[23] It can be mentioned that the exponents in Table I (or even the effective exponents in Fig. 9) are not consistent with that for dipolar-FM,[26] so we have attempted to explain the spin interaction in PSMO based on the latter model. According to this model, the range of spin interaction is long or short depending on the $\sigma < 2$ or $\sigma > 2$, and it predicts the susceptibility exponent γ which has been calculated from renormalization group approach, as following.

$$\gamma = 1 + \frac{4}{d}\left(\frac{n+2}{n+8}\right)\Delta\sigma + \frac{8(n+2)(n-4)}{d^2(n+8)^2} \times \left[1 + \frac{2G\left(\frac{d}{2}\right)(7n+20)}{(n-4)(n+8)}\right]\Delta\sigma^2,$$

where $\Delta\sigma = (\sigma - \frac{d}{2})$ and $G(\frac{d}{2}) = 3 - \frac{1}{4}(\frac{d}{2})^2$.

To find out the range of interaction (σ) as well as the dimensionality of both lattice (d) and spin (n) in this system we have followed the procedure similar to Ref. 37 where the parameter σ in above expression is adjusted for a particular values of $\{d:n\}$ so that it yields a value for γ close to that observed experimentally (1.334). The so obtained σ is then used to calculate the remaining exponents from the following expressions: $\nu = \gamma/\sigma$, $\alpha = 2 - \nu d$, $\beta = (2 - \alpha - \gamma)/2$, and $\delta = 1 + \gamma/\beta$. This exercise is repeated for different set of $\{d:n\}$. We found that $\{d:n\} = \{2:3\}$ and $\sigma = 1.252$ give the exponents ($\beta = 0.397$, $\gamma = 1.331$, and $\delta = 4.35$) which are close to our experimentally observed values (Table I). This calculation suggests the spin interaction in this compound is of 2D Heisenberg ($\{d:n\} = \{2:3\}$) type coupled with long-range ($\sigma = 1.252$) interaction. This result is apparently counter intuitive. Nonetheless, it indicates that effective dimensionally of spin interaction is <3, and the range of interaction extends beyond the nearest neighbors.

This situation is probably justified for PSMO considering its A-type AF ground state where FM planes are coupled antiferromagnetically. Even though at high T system attains fully FM ordering but the spin interaction is reminiscent of low T phase, exhibiting a tendency toward 2D character. The ferromagnetism in this class of materials is explained through DE mechanism which assumes the coupling of itinerant e_g electrons with the localized t_{2g} electrons. This may lead to a situation where the interaction extends beyond the nearest neighbors. Furthermore, PSMO shows phase separation with the formation of FM and AF clusters just below T_C, and FM clusters are also evident above T_C in this compound.[21] This phase inhomogeneity both below and above T_C in PSMO will have considerable influence on the critical behavior. The change in shape and size of FM clusters with temperature around T_C can lead to effective dimensionality of spin interaction <3. In general, critical exponents for inhomogeneous ferromagnetic systems are inconsistent with conventional universality classes. For example, large value of $\beta(0.43 \rightarrow 0.46)$ are found due to phase segregation in $La_{1-x}Sr_xCoO_3$ compound.[12] Similarly, $\beta = 0.57(1)$ and $\gamma = 1.16(3)$ are found for single crystal of $Nd_{0.7}Sr_{0.3}MnO_3$ due to formation of FM clusters above T_C.[13] In another study, unusual exponents [$\delta = 20(1)$, $\beta = 0.09(1)$, and $\gamma = 1.71(1)$] are observed for $La_{0.79}Ca_{0.21}MnO_3$ as a result of Griffiths phase formation.[14] Other than perovskites, $Gd_{80}Au_{20}$ also shows unusual exponents [$\beta = 0.44(2)$ and $\gamma = 1.29(5)$] arising from dilution of global spin due to nonmagnetic ion substitution.[39] Thus, these results suggest that critical phenomenon in inhomogeneous systems could not be explained on the basis of existing universality classes. Probably, they constitute a separate class. However, further experimental studies accompanied by theoretical calculations are required to generalize this observation.

V. CONCLUSION

In conclusion, we have made a comprehensive study on the critical phenomenon at the PM-FM phase transition in double exchange driven ferromagnetic material $Pr_{0.5}Sr_{0.5}MnO_3$. This transition is identified to be second order in nature. The critical exponents β, γ, and δ estimated from various techniques match reasonably well and values are in between those theoretically predicted for 3D Heisenberg and mean-field interaction models. It is significant that even with these critical exponents; magnetization, field, and temperature (M-H-T) data follow the scaling equation where they collapse into two distinct branches: one below T_C and

another above T_C. This conclusively shows that calculated critical exponents as well as critical temperature are unambiguous and intrinsic to the system. The temperature variation in the effective exponents (β_{eff} and γ_{eff}) of this compound are similar to those for disordered ferromagnet. For $Pr_{0.5}Sr_{0.5}MnO_3$, disorder can arise from size mismatch of Pr^{3+} and Sr^{2+} ions. However, this disorder has also the possibility to induce Griffiths phaselike properties, and whether the observed nature of exponents is related to such phenomenon is to be verified. It is observed that fully localized spin-interaction models are not applicable for this compound, and ferromagnetism is having of itinerant character. The exponents determined in this study are close to the values calculated from renormalization group approach for 2D Heisenberg model coupled with long range interaction. This situation is probably justified for this compound with *A*-type AF ground state having FM interaction along the planes. Moreover, the inhomogeneous magnetic state both below and above T_C may have serious consequences on critical behavior. This study points toward the fact that critical phenomenon in disordered ferromagnets could not be tackled with the common universality classes, indicating perhaps they represent separate class. This should prompt further experimental studies followed by rigorous theoretical works.

ACKNOWLEDGMENTS

DST, Government of India is acknowledged for funding VSM. A.K.P also acknowledges CSIR, India for financial assistance.

[1] Sunil Nair, A. Banerjee, A. V. Narlikar, D. Prabhakaran, and A. T. Boothroyd, Phys. Rev. B **68**, 132404 (2003).
[2] K. Ghosh, C. J. Lobb, R. L. Greene, S. G. Karabashev, D. A. Shulyatev, A. A. Arsenov, and Y. Mukovskii, Phys. Rev. Lett. **81**, 4740 (1998).
[3] J. W. Lynn, R. W. Erwin, J. A. Borchers, Q. Huang, A. Santoro, J.-L. Peng, and Z. Y. Li, Phys. Rev. Lett. **76**, 4046 (1996).
[4] J. Mira, J. Rivas, F. Rivadulla, C. Vazquez-Vazquez, and M. A. Lopez-Quintela, Phys. Rev. B **60**, 2998 (1999).
[5] X. Z. Zhou, H. P. Kunkel, J. H. Zhao, P. A. Stampe, and Gwyn Williams, Phys. Rev. B **56**, R12714 (1997).
[6] C. Zener, Phys. Rev. **82**, 403 (1951).
[7] K. Kubo and N. Ohata, J. Phys. Soc. Jpn. **33**, 21 (1972).
[8] Y. Motome and N. Furukawa, J. Phys. Soc. Jpn. **69**, 3785 (2000); **70**, 1487 (2001).
[9] J. L. Alonso, L. A. Fernández, F. Guinea, V. Laliena, and V. Martín-Mayor, Nucl. Phys. B **596**, 587 (2001).
[10] A. Moreo, Seiji Yunoki, and Elbio Dagotto, Science **283**, 2034 (1999); E. Dagotto, *Nanoscale Phase Separation and Colossal Magnetoresistance* (Springer, New York, 2002).
[11] J. M. De Teresa, M. R. Ibarra, P. A. Algarabel, C. Ritter, C. Marquina, J. Balasco, J. Garcia, A. del Moral, and Z. Arnold, Nature (London) **386**, 256 (1997).
[12] J. Mira, J. Rivas, M. Vazquez, J. M. Garcia-Beneytez, J. Arcas, R. D. Sańchez, and M. A. Señaris-Rodriguez, Phys. Rev. B **59**, 123 (1999).
[13] R. Venkatesh, M. Pattabiraman, S. Angappane, G. Rangarajan, K. Sethupathi, J. Karatha, M. Fecioru-Morariu, R. M. Ghadimi, and G. Guntherodt, Phys. Rev. B **75**, 224415 (2007).
[14] W. Jiang, X. Z. Zhou, G. Williams, Y. Mukovskii, and K. Glazyrin, Phys. Rev. Lett. **99**, 177203 (2007).
[15] R. B. Griffiths, Phys. Rev. Lett. **23**, 17 (1969).
[16] P. Y. Chan, N. Goldenfeld, and M. Salamon, Phys. Rev. Lett. **97**, 137201 (2006).
[17] Y. Tomioka, A. Asamitsu, Y. Moritomo, H. Kuwahara, and Y. Tokura, Phys. Rev. Lett. **74**, 5108 (1995).
[18] H. Kawano, R. Kajimoto, H. Yoshizawa, Y. Tomioka, H. Kuwahara, and Y. Tokura, Phys. Rev. Lett. **78**, 4253 (1997).
[19] R. Kajimoto, H. Yoshizawa, Y. Tomioka, and Y. Tokura, Phys. Rev. B **66**, 180402(R) (2002).
[20] A. Banerjee, A. K. Pramanik, Kranti Kumar, and P. Chaddah, J. Phys.: Condens. Matter **18**, L605 (2006).
[21] A. K. Pramanik and A. Banerjee, J. Phys.: Condens. Matter **20**, 275207 (2008).
[22] S. Cao, B. Kang, J. Zhang, and S. Yuan, Appl. Phys. Lett. **88**, 172503 (2006).
[23] M. E. Fisher, Shang-keng Ma, and B. G. Nickel, Phys. Rev. Lett. **29**, 917 (1972).
[24] H. E. Stanley, *Introduction to phase transitions and critical phenomenon* (Oxford University Press, New York, 1971).
[25] A. Perumal, V. Srinivas, V. V. Rao, and R. A. Dunlap, Phys. Rev. Lett. **91**, 137202 (2003).
[26] S. Srinath, S. N. Kaul, and M.-K. Sostarich, Phys. Rev. B **62**, 11649 (2000), and references therein.
[27] A. Arrott, Phys. Rev. **108**, 1394 (1957).
[28] S. K. Banerjee, Phys. Lett. **12**, 16 (1964).
[29] Anthony Arrott and John E. Noakes, Phys. Rev. Lett. **19**, 786 (1967).
[30] A. Aharoni, *Introduction to the Theory of Ferromagnetism* (Clarendon Press, Oxford, 1996), Chap. 4.
[31] J. S. Kouvel and M. E. Fisher, Phys. Rev. **136**, A1626 (1964).
[32] B. Widom, J. Chem. Phys. **43**, 3898 (1965); J. Chem. Phys. **41**, 1633 (1964).
[33] S. N. Kaul, J. Magn. Magn. Mater. **53**, 5 (1985).
[34] M. Dudka, R. Folk, Yu. Holovatch, and D. Ivaneiko, J. Magn. Magn. Mater. **256**, 243 (2003).
[35] P. Rhodes and E. P. Wohlfarth, Proc. R. Soc. London **273**, 247 (1963).
[36] E. P. Wohlfarth, J. Magn. Magn. Mater. **7**, 113 (1978).
[37] S. F. Fischer, S. N. Kaul, and H. Kronmüller, Phys. Rev. B **65**, 064443 (2002).
[38] Amnon Aharony and Michael E. Fisher, Phys. Rev. B **8**, 3323 (1973); Alastair D. Bruce and Amnon Aharony, *ibid.* **10**, 2078 (1974); K. Ried, Y. Millev, M. Fähnle, and H. Kronmüller, *ibid.* **51**, 15229 (1995).
[39] S. J. Poon and J. Durand, Phys. Rev. B **16**, 316 (1977).